Molecular BioSystems c4mb00747f

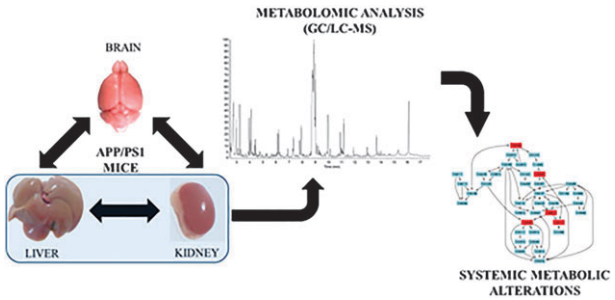

Metabolomic investigation of systemic manifestations associated with Alzheimer's disease in the APP/PS1 transgenic mouse model

Raúl González-Domínguez, Tamara García-Barrera, Javier Vitorica and José Luis Gómez-Ariza*

This work describes the first metabolomic investigation of systemic manifestations of Alzheimer's disease in liver and kidney from the APP/PS1 transgenic mouse model.

Q2

Please check this proof carefully. **Our staff will not read it in detail after you have returned it.**

Translation errors between word-processor files and typesetting systems can occur so the whole proof needs to be read. Please pay particular attention to: tabulated material; equations; numerical data; figures and graphics; and references. If you have not already indicated the corresponding author(s) please mark their name(s) with an asterisk. Please e-mail a list of corrections or the PDF with electronic notes attached – do not change the text within the PDF file or send a revised manuscript. Corrections at this stage should be minor and not involve extensive changes. All corrections must be sent at the same time.

Please bear in mind that minor layout improvements, e.g. in line breaking, table widths and graphic placement, are routinely applied to the final version.

Please note that, in the typefaces we use, an italic vee looks like this: v, and a Greek nu looks like this: ν.

We will publish articles on the web as soon as possible after receiving your corrections; **no late corrections will be made.**

Please return your **final** corrections, where possible within **48 hours** of receipt, by e-mail to: molbiosyst@rsc.org

Queries for the attention of the authors

Journal: **Molecular BioSystems**

Paper: **c4mb00747f**

Title: **Metabolomic investigation of systemic manifestations associated with Alzheimer's disease in the APP/PS1 transgenic mouse model**

Editor's queries are marked on your proof like this Q1, Q2, etc. and for your convenience line numbers are indicated like this 5, 10, 15, ...

Please ensure that all queries are answered when returning your proof corrections so that publication of your article is not delayed.

Query reference	Query	Remarks
Q1	For your information: You can cite this article before you receive notification of the page numbers by using the following format: (authors), Mol. BioSyst., (year), DOI: 10.1039/c4mb00747f.	
Q2	Please carefully check the spelling of all author names. This is important for the correct indexing and future citation of your article. No late corrections can be made.	

Molecular BioSystems

PAPER

Metabolomic investigation of systemic manifestations associated with Alzheimer's disease in the APP/PS1 transgenic mouse model

Raúl González-Domínguez,[abc] Tamara García-Barrera,[abc] Javier Vitorica[def] and José Luis Gómez-Ariza*[abc]

Cite this: DOI: 10.1039/c4mb00747f

Received 26th December 2014,
Accepted 5th June 2015

DOI: 10.1039/c4mb00747f

www.rsc.org/molecularbiosystems

There is growing evidence that Alzheimer's disease may be a widespread systemic disorder, so peripheral organs could be affected by pathological mechanisms occurring in this neurodegenerative disease. For this reason, a double metabolomic platform based on the combination of gas chromatography-mass spectrometry and ultra-high performance liquid chromatography-mass spectrometry was used for the first time to investigate metabolic changes in liver and kidney from the transgenic mice APP/PS1 against wild-type controls. Multivariate statistics showed significant differences in levels of numerous metabolites including phospholipids, sphingolipids, acylcarnitines, steroids, amino acids and other compounds, which denotes that multiple pathways might be associated with systemic pathogenesis of Alzheimer's in this mouse model, such as bioenergetic failures, oxidative stress, altered metabolism of membrane lipids, hyperammonemia or impaired homeostasis of steroids. Furthermore, it is noteworthy that some novel pathological mechanisms were found, such as impaired gluconeogenesis, polyol pathway or metabolism of branched chain amino acids, not previously described for Alzheimer's disease. Therefore, these findings clearly support the hypothesis that Alzheimer's disease may be considered as a systemic disorder.

1. Introduction

Nowadays, the understanding of pathological mechanisms occurring in Alzheimer's disease (AD) is a primary topic in biomedical research. Although the initiating events are still unknown, this neurodegenerative disorder seems to have a multifactorial origin that involves profound biochemical alterations in multiple pathways in the brain. Thereby, pathogenesis of AD has been predominantly associated with deposition of senile plaques containing β-amyloid peptides and formation of neurofibrillary tangles in the brain,[1] combined with other neuronal impairments such as oxidative stress,[2] neuroinflammation[3] or mitochondrial dysfunction,[4] among others. However, there is growing evidence that Alzheimer's disease may be a widespread systemic disorder, so pathological lesions could be not only localized in the brain. In this sense, Joachim *et al.* demonstrated that deposition of amyloid-β peptides can be found in different non-neural tissues,[5] which has been confirmed in more recent studies in a wide variety of organs.[6] Moreover, other key hallmarks of AD also occur outside the central nervous system affecting peripheral organs, such as inflammation,[7] oxidative stress[8] and metabolic dysfunction.[9] The crucial role that altered metal homeostasis plays in the development of Alzheimer's disease is also noteworthy, contributing to Aβ deposition, oxidative stress production and other pathological processes.[10,11] Disturbances of metal metabolism might occur at several biological pathways, including uptake and release, storage, intracellular metabolism, and their regulation. For this reason, metal dyshomeostasis in AD should be viewed within a wide framework of systemic alterations in metal management.[12] Thus, the study of other tissues rather than brain may provide a new insight into pathological mechanisms occurring in Alzheimer's disease. Particularly important are liver and kidney, the most metabolically active organs involved in different functions such as detoxification, regulatory processes and production of biochemicals. Alzheimer's disease has been associated with liver failures related to impaired biosynthesis of essential compounds operating in the

[a] Department of Chemistry and CC.MM, Faculty of Experimental Sciences, University of Huelva, Campus de El Carmen, 21007 Huelva, Spain. E-mail: ariza@uhu.es; Fax: +34 959 219942; Tel: +34 959 219968
[b] Campus of Excellence International ceiA3, University of Huelva, Spain. E-mail: tamara@dqcm.uhu.es; Fax: +34 959 219942; Tel: +34 959 219962
[c] Research Center of Health and Environment (CYSMA), University of Huelva, Campus de El Carmen, 21007 Huelva, Spain
[d] Department Bioquímica, Bromatologia, Toxicología y Medicina Legal, Faculty of Pharmacy, University of Seville, 41012 Seville, Spain
[e] Centro de Investigación Biomédica en Red sobre Enfermedades Neurodegenerativas (CIBERNED), 41013 Seville, Spain
[f] Instituto de Biomedicina de Sevilla (IBiS)–Hospital Universitario Virgen del Rocío/CSIC/University of Seville, 41013 Seville, Spain

brain, including docosahexaenoic acid,[13] glutathione,[14] and plasmalogens.[15] On the other hand, perturbed kidney function can also be linked to cognitive impairments through small vessel disease,[16] in relation to impaired regulation of the rennin–angiotensin system leading to hypertension. Therefore, the application of a holistic approach for the characterization of peripheral abnormalities in Alzheimer's disease may be of great interest.

In this work, for the first time we performed a metabolomic investigation into systemic alterations associated with Alzheimer's disease in peripheral tissues (liver and kidney) from the double transgenic mouse model APP/PS1. This model reproduces some of the neuropathological and cognitive deficits observed in AD, with a phenotype characterized by early amyloid deposits and behavioral deficits,[17] and exhibits profound abnormalities in the neurochemical profile.[18,19] In order to obtain a comprehensive understanding about pathological mechanisms occurring in the APP/PS1 mice, we used a high-throughput metabolomic approach combining gas chromatography-mass spectrometry (GC-MS) and reversed-phase ultra-high performance liquid chromatography-mass spectrometry (UHPLC-MS). This multiplatform methodology allows extending the analytical coverage of endogenous metabolites because of the complementarity of the different profiling techniques. Thereby, while GC-MS provides high-chromatographic resolution for primary low molecular weight metabolites, reversed phase chromatography can be considered as the standard tool for the separation of medium polar and non-polar analytes.[20] Finally, multivariate statistics was used to identify metabolites responsible for discrimination and to elucidate affected biochemical pathways.

2. Materials and methods

2.1. Animal handling

Transgenic APP/PS1 mice (C57BL/6 background) were generated as previously described by Jankowsky *et al.*, expressing the Swedish mutation of APP together with PS1 deletion in exon 9.[21] On the other hand, age-matched wild-type mice of the same genetic background (C57BL/6) were purchased from Charles River Laboratory for their use as controls. In this study, male and female animals at 6 months of age were used for experiments (TG: N = 30, male/female 13/17; WT: N = 30, male/female 15/15). Animals were acclimated for 3 days after reception in rooms with a 12 h light–dark cycle at 20–25 °C, with water and food available *ad libitum*. Then, mice were anesthetized by isoflurane inhalation and sacrificed by exsanguination *via* cardiac puncture. Liver and kidneys were rapidly removed, rinsed with saline solution (0.9% NaCl w/v), snap-frozen in liquid nitrogen and stored at −80 °C until analysis. Animals were handled according to the directive 2010/63/EU stipulated by the European Community, and the study was approved by the Ethical Committee of University of Huelva.

2.2. Tissue extraction

Liver and kidneys were cryo-homogenized using a cryogenic homogenizer SPEX SamplePrep (Freezer/Mills 6770), for 30 seconds at rate of 10 strokes per second. Subsequently, tissues were extracted with pre-cooled 0.1% formic acid in methanol (−20 °C) using a pellet mixer for cell disruption (VWR International, UK) as described elsewhere.[18] For this, 30 mg of tissue samples were exactly weighed in Eppendorf tubes and mixed with 300 μL of the extraction solvent. The mixture was homogenized for 2 min in an ice bath, and then centrifuged at 10 000 rpm for 10 min at 4 °C. An aliquot of the supernatant (50 μL) was split for derivatization before GC-MS fingerprinting, and the rest of the sample was transferred to the injection vial for UHPLC-MS analysis. Derivatization was carried out according to a two-step methodology based on oximation and silylation. For this, 50 μL of extracts were dried under nitrogen stream and redissolved in 50 μL of 20 mg mL^{-1} methoxyamine in pyridine for protection of carbonyl groups during methoximation. After briefly vortexing, samples were incubated at 80 °C for 15 min in a water bath. Then silylation was performed by adding 50 μL of MSTFA (*N*-methyl-*N*-trimethylsilyl trifluoroacetamide) and incubating at 80 °C for a further 15 min. Finally, extracts were centrifuged at 4000 rpm for one minute and the supernatant was collected for analysis. Furthermore, quality control (QC) samples were prepared by pooling equal volumes of each sample, which allows monitoring the stability and performance of the system along the period of analysis.[22]

2.3. Metabolomic profiling by GC-MS

Analyses were performed using a Trace GC ULTRA gas chromatograph coupled to an ion trap mass spectrometer detector ITQ 900 (Thermo Fisher Scientific), and a factor four capillary column VF-5MS 30 m × 0.25 mm ID, with 0.25 μm of film thickness (Varian). The GC column temperature was set to 100 °C for 0.5 minutes, and programmed to reach 320 °C at a rate of 15 °C per minute. Finally, this temperature was maintained for a further 2.8 minutes, with the total time of analysis being 18 minutes. The injector temperature was kept at 280 °C, and helium was used as a carrier gas at a constant flow rate of 1 mL min^{-1}. For mass spectrometry detection, ionization was carried out by electronic impact (EI) using a voltage of 70 eV, and the ion source temperature was set at 200 °C. Data were obtained acquiring full scan spectra in the m/z range 35–650. For analysis, 1 μL of sample was injected in the splitless mode.

2.4. Metabolomic profiling by UHPLC-MS

Samples were fingerprinted using an ultra-high performance liquid chromatograph (Accela LC system, Thermo Fisher Scientific) coupled to a quadrupole-time-of-flight mass spectrometry system equipped with electrospray source (QSTAR XL Hybrid system, Applied Biosystems). Chromatographic separations were performed using a reversed-phase column (Hypersil Gold C18, 2.1 × 50 mm, 1.9 μm) thermostated at 50 °C, with an injection volume of 5 μL. Solvents were delivered at a flow rate 0.5 mL min^{-1}, using methanol (solvent A) and water (solvent B), both containing 10 mM ammonium formate and 0.1% formic acid. The gradient elution program was: 0–1 min, 95% B; 2.5 min, 25% B; 8.5–10 min, 0% B; 10.1–12 min, 95% B. MS operated in positive and negative polarities, acquiring full scan

spectra in the *m/z* range 50–1000 with 1.005 seconds scan time. The ion spray voltage (IS) was set at 5000 V and −2500 V, and high-purity nitrogen was used as a curtain, a nebulizer and heater gas at flow rates of about 1.48 L min^{-1}, 1.56 L min^{-1} and 6.25 L min^{-1}, respectively. The source temperature was fixed at 400 °C, with a declustering potential (DP) of 100 V/−120 V, and a focusing potential (FP) of ±350 V. To acquire MS/MS spectra, nitrogen was used as the collision gas.

2.5. Data processing

Raw data were processed following the pipeline described by Katajamaa *et al.*, which proceeds through multiple stages including feature detection, alignment of peaks and normalization.[23] For this purpose, we employed the freely available software XCMS, included in the R platform (http://www.r-project.org). UHPLC-MS files were converted into the mzXML format using the msConvert tool (ProteoWizard), while GC-MS files were converted into netCDF using the Thermo File Converter tool (Thermo Fisher Scientific). Subsequently, data were extracted using the matchedFilter method. This algorithm slices data into extracted ion chromatograms (XIC) on a fixed step size (default 0.1 *m/z*), and then each slice is filtered with matched filtration using a second-derivative Gaussian as the model peak shape.[24] The XCMS parameters were optimized according to the characteristics of data sets obtained in order to extract the maximum information possible. Finally, the settings applied for UHPLC-MS data were S/N threshold 2 and full width at half-maximum (fwhm) 10, while for GC-MS data the fwhm was set at 3. After peak extraction, grouping and retention time correction of peaks (alignment) were accomplished in three iterative cycles with descending bandwidth (bw) from 10 to 1 second in UHPLC-MS, and descending bw from 5 to 1 second for GC-MS. Then, imputation of missing values was performed by returning to the raw spectral data and integrating the areas of the missing peaks which are below the applied signal-to-noise ratio threshold, using the fillPeaks algorithm. For data normalization, the locally weighted scatter plot smoothing (LOESS) normalization method was used, which adjusts the local median of log fold changes of peak intensities between samples in the data set to be approximately zero across the whole peak intensity range.[25] Finally, data were submitted to logarithmic transformation, in order to stabilize the variance of results. The preprocessed data were then exported as a csv file for further data analysis by multivariate procedures.

2.6. Data analysis

Data were subjected to multivariate analysis by principal component analysis (PCA) and partial least squares discriminant analysis (PLS-DA) in order to compare metabolomic profiles obtained, using the SIMCA-P™ software (version 11.5, UMetrics AB, Umeå, Sweden). Before performing statistical analysis, data were submitted to Pareto scaling, for reducing the relative importance of larger values.[26] Quality of the models was assessed by the R^2 and Q^2 values, supplied by the software, which provide information about the class separation and predictive power of the model, respectively. These parameters are ranged between 0 and 1, and they indicate the variance explained by the model for all the data analyzed (R^2) and this variance in a test set by cross-validation (Q^2). Finally, potential biomarkers were selected according to the variable importance in the projection, or VIP (a weighted sum of squares of the PLS weight, which indicates the importance of the variable in the model), considering only variables with VIP values higher than 1.5, indicative of significant differences among groups. These metabolites were validated by the *t*-test with Bonferroni correction for multiple testing (*p*-values below 0.05), using the STATISTICA 8.0 software (StatSoft, Tulsa, USA).

2.7. Identification of metabolites

Potential biomarkers detected by GC-MS were identified using the NIST Mass Spectral Library (version 08), considering only those variables with a similarity index (SI) greater than 90%. Alternatively, identification of metabolites from UHPLC-MS profiling was made matching the experimental accurate mass and tandem mass spectra (MS/MS) with those available in metabolomic databases (HMDB, METLIN and LIPIDMAPS). Furthermore, the identity of lipids detected by this latter technique was confirmed based on fragmentation patterns described in the literature. Phosphocholines (PC) presented characteristic ions in the positive ionization mode at *m/z* 184, 104 and 86, and two typical fragments due to the loss of trimethylamine (*m/z* 59) and phosphocholine (*m/z* 183). In contrast, the product-ion spectra of ethanolamines (PE) and serines (PS) were dominated by $[M + H\text{-}141]^+$ and $[M + H\text{-}185]^+$ respectively, arising from the elimination of the phosphoethanolamine or phosphoserine moiety. Finally, in the negative mode these distinctive signals were found at 168, 196, 241, 171 and $[M\text{-}H\text{-}87]^-$, for choline (PC), ethanolamine (PE), inositol (PI), glycerol (PG) and serine (PS) derived lipids, respectively. Furthermore, the fragmentation in the glycerol backbone and release of the fatty acyl substituents enabled the identification of individual species of phospholipids, as previously described.[27] For sphingolipids (sphingomyelins, SM, and ceramides, CER) typical product ions appear at *m/z* 264 and 282 due to the fragmentation in the sphingosine moiety, and the cleavage of the phosphocholine headgroup from sphingomyelins generates characteristic fragments at 184 and 168 *m/z*, in positive and negative modes, respectively.[28] Finally, acylcarnitines were confirmed based on characteristic fragments of *m/z* 60 and 85.[29]

3. Results and discussion

3.1. Metabolomic profiling of tissue samples

Liver and kidney samples from APP/PS1 and wild type mice were fingerprinted by using a high-throughput metabolomic approach based on simple tissue homogenization and fast analysis by complementary gas chromatography-mass spectrometry (total analysis time: 18 min) and reversed-phase ultra-high performance liquid chromatography-mass spectrometry (total analysis time: 12 min). This multi-platform allowed the

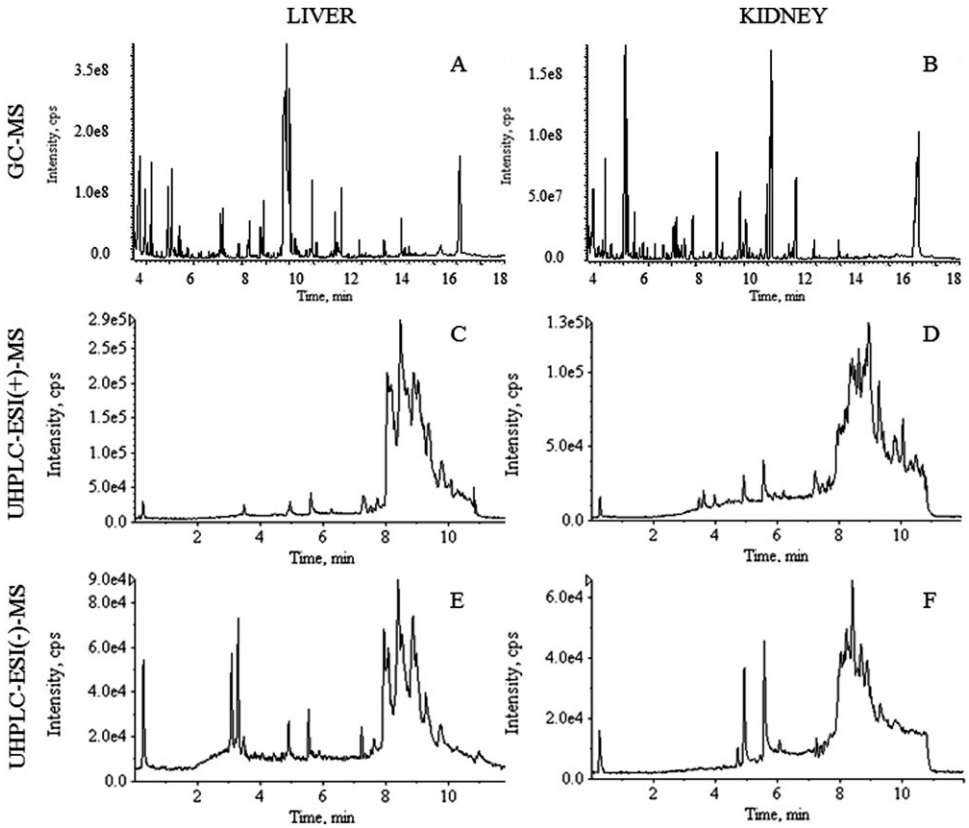

Fig. 1 Total ion chromatograms for liver and kidney extracts analyzed by GC-MS (A and B), UHPLC-ESI(+)-MS (C and D) and UHPLC-ESI(−)-MS (E and F).

detection of numerous metabolic features, as can be observed in corresponding chromatograms (Fig. 1). After peak detection, alignment, grouping and normalization using XCMS, *ca.* 5000 molecular features were detected in UHPLC-MS profiles (in each ion mode), and 2000 peaks were obtained from GC-MS analysis. Moreover, quality control samples (QC) were employed in order to validate the analytical performance of this method.[30] QC samples were prepared by pooling equal volumes from each individual sample, and then were analyzed at the start of the run in order to equilibrate the analytical system as well as at intermittent points throughout the sequence to monitor the robustness of the technique. The relative standard deviation of peak areas in QC samples was less than 12% for all metabolites identified in this study (as detailed in Section 3.2), indicative of an excellent reproducibility in accordance with the criteria defined by the US Food and Drug Administration.[31] Furthermore low RSD values were observed for retention times before alignment (below 1%), demonstrating the instrumental stability of this metabolomic approach, which facilitates subsequent data processing. Therefore, it can be concluded that the metabolomic multiplatform used in this study presents a great potential for comprehensive metabolite profiling of tissue samples, considering the high number of molecular features detected and the good reproducibility measured in QC samples in terms of signal intensity and retention time. Thereby, after raw data pre-processing, the final data matrix was subjected to multivariate statistical analysis in order to perform sample classification and determine metabolic abnormalities associated with AD-type disorders in liver and kidney of the APP/PS1 mouse model.

3.2. Multivariate statistics

Before performing multivariate analysis, the data matrix containing the time-aligned peaks was subjected to logarithmic transformation and Pareto scaling in order to extract relevant biological information from these large data sets, reducing the technical variability between individual samples.[26] Principal component analysis (PCA) was firstly applied to detect possible outliers and to ensure grouping of quality control samples. A good clustering of QCs was observed in the score plot (Fig. 2A and B, for liver and kidney), indicative of stability during the analyses,[22] without significant outliers according to the Hotelling T^2-range plot (not shown). Supervised partial least-squares discriminant analysis (PLS-DA) demonstrated a perfect discrimination between transgenic mice and control animals (Fig. 2C and D, for liver and kidney). These models yielded satisfactory values for the quality parameters R^2 and Q^2, with a variance explained close to 100% and variance predicted above 65% for data from GC-MS, UHPLC-ESI(+)-MS and UHPLC-ESI(−)-MS (Table 1). Then, metabolites influencing the differentiation between APP/PS1 and wild type mice were identified as previously described (Section 2.7). These discriminant compounds are listed in Tables 2–4 along with the retention time, the ionization mode used for detection (P: positive ions in UHPLC-MS; N: negative ions in UHPLC-MS; EI: electronic

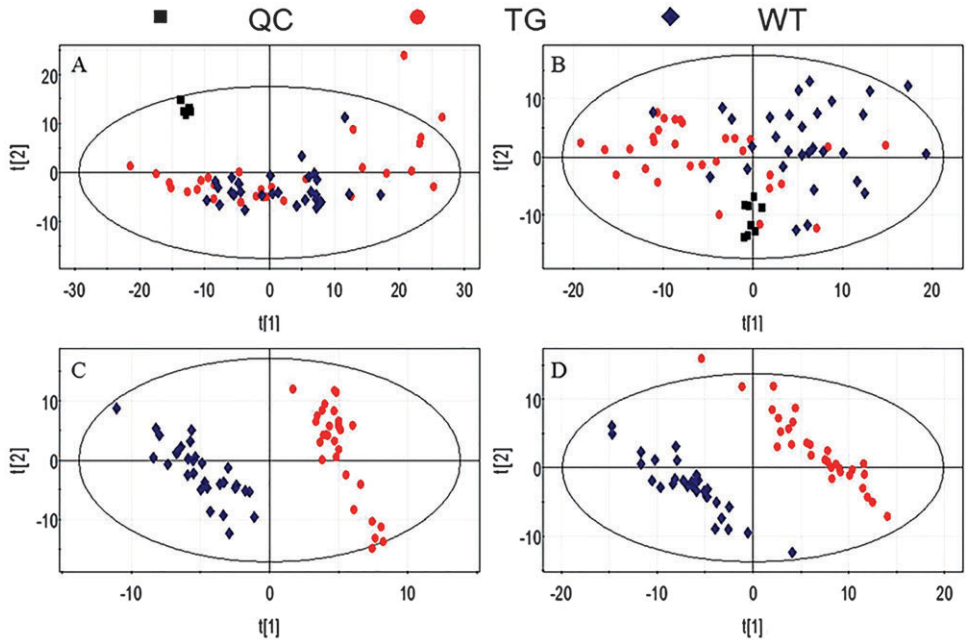

Fig. 2 Score plots of statistical models for UHPLC-ESI(+)-MS data. (A) PCA for liver; (B) PCA for kidney; (C) PLS-DA for liver; (D) PLS-DA for kidney.

Table 1 Statistical parameters of PLS-DA models for liver and kidney. *A*: number of latent components; R^2: variance explained; Q^2: variance predicted

		Liver	Kidney
GC/MS	*A*	3	3
	R^2	0.994	0.996
	Q^2	0.681	0.659
UHPLC-ESI(+)/MS	*A*	5	5
	R^2	0.99	0.988
	Q^2	0.867	0.916
UHPLC-ESI(−)/MS	*A*	5	5
	R^2	0.995	0.995
	Q^2	0.963	0.899

impact in GC-MS), the fold change (calculated by dividing the mean area for peaks in the APP/PS1 group by the mean area in the control group) and the *p*-value for each tissue, and the relative standard deviation observed in QC samples. Levels of numerous lipids were significantly altered in both liver and kidney, including phospholipids and lyso-phospholipids (Table 2), sphingolipids, steroids, acylcarnitines and fatty acids (Table 3), showing the potential of reversed-phase ultra-high performance liquid chromatography-mass spectrometry for comprehensive lipidomic profiling. On the other hand, GC-MS results demonstrated the implication of different low molecular weight metabolites in pathogenesis of AD-type disorders in this mouse model, which was complemented with several polar compounds detected by UHPLC-MS in the void volume (Table 4). Moreover, the similarities found in both tissues in terms of up- or down-expression for most of these marker metabolites are noteworthy, suggesting common perturbed pathways affecting the whole organism in response to AD impairments, as discussed in the next section.

On the other hand, we also investigated the effect of gender in metabolite differences detected in this study in order to consider its contribution to variability in metabolomic profiles. A balanced number of males and females were comprised within each group (*i.e.* wild type and transgenic animals) in order to reduce gender-related differences. Thereby, similar metabolites were detected for WT-APP/PS1 discrimination when each gender was modeled separately by PLS-DA (Fig. 3A–D), thus demonstrating that the effect of gender on metabolic profiles is much less important that the diseased state. Furthermore, we also performed *t*-tests according to gender for discriminant metabolites presented in Tables 2–4, and *p*-values obtained were much lower to those listed in previous tables for the comparison of APP/PS1 *vs.* WT (Fig. 3E). Only a few metabolites presented a statistically different trend between male and female mice, principally some phospholipids and carnitine-derived compounds, probably as a consequence of endocrine disruption, as previously described in mice dietary exposed to phthalates and polychlorinated biphenyls.[32] Therefore, it could be concluded that metabolic differences arising from gender are not as important for sample discrimination as those related to the presence of the disease.

3.3. Biological meaning

Metabolomics has demonstrated a great potential in Alzheimer's disease research due to its feasibility to deal with the full complexity of the disease phenotype. Thereby, metabolomic analysis of brain samples has been extensively applied to examine neurochemical perturbations involved in pathological mechanisms occurring in AD, in both humans[33,34] and transgenic mice.[35–37] On the other hand, other metabolomic approaches

Table 2 Phospholipids identified as potential markers for discrimination between APP/PS1 and control mice

			Liver		Kidney		
Metabolite	RT (min)	Ion mode	Fold change	*p*-value	Fold change	*p*-value	RSD (%)
Lyso-phospholipids							
LPC(18 : 2)	4.67	N	—	—	0.79	4.2×10^{-2}	6.9
LPS(18 : 0)	4.95	N	—	—	1.21	1.7×10^{-2}	3.1
LPC(18 : 1)	5.08	P, N	0.61	1.2×10^{-3}	0.77	4.4×10^{-2}	4.5
LPE(18 : 0)	5.23	P	1.53	1.3×10^{-2}	—	—	4.3
LPC(18 : 0)	5.67	P, N	1.59	9.9×10^{-4}	1.59	3.9×10^{-2}	3.5
Phospholipids							
PG(22 : 6/22 : 6)	6.92	N	—	—	1.64	4.1×10^{-2}	7.1
PS(22 : 6/22.4)	6.95	P	0.65	1.9×10^{-2}	1.29	3.2×10^{-2}	8.9
PG(18 : 2/22 : 6)	6.98	N	—	—	1.74	3.4×10^{-2}	10.6
PG(18 : 2/20 : 4)	7.02	N	—	—	1.37	4.2×10^{-2}	3.1
PG(18 : 2/18 : 2)	7.03	N	—	—	1.57	3.8×10^{-2}	2.9
PG(18 : 1/22 : 6)	7.25	N	0.44	2.6×10^{-2}	1.47	3.5×10^{-2}	7.4
PG(18 : 2/18 : 1)	7.32	N	—	—	1.21	3.8×10^{-2}	1.1
PI(18 : 2/18 : 1)	7.52	N	—	—	1.28	2.4×10^{-2}	6.8
PI(16 : 0/18 : 2)	7.53	N	—	—	1.33	8.7×10^{-3}	6.9
PE(16 : 1/22 : 6)	7.60	P, N	0.68	4.2×10^{-3}	0.87	4.4×10^{-2}	8.0
PE(16 : 1/20 : 4)	7.67	P, N	0.62	5.8×10^{-3}	0.76	3.9×10^{-2}	5.3
PS(16 : 0/20 : 4)	7.75	P	0.44	3.7×10^{-2}	—	—	7.8
PI(16 : 0/18 : 1)	7.78	N	—	—	1.36	9.1×10^{-4}	4.1
PE(16 : 1/16 : 0)	7.88	N	—	—	0.81	4.0×10^{-2}	1.1
PE(16 : 0/22 : 6)	7.93	N	—	—	0.93	3.4×10^{-2}	3.2
PI(18 : 2/18 : 0)	7.93	N	—	—	1.38	5.7×10^{-4}	4.6
PE(16 : 0/20 : 3)	7.98	N	—	—	0.96	4.1×10^{-2}	5.4
PE(18 : 1/22 : 6)	8.02	P, N	0.72	4.3×10^{-3}	0.91	3.6×10^{-2}	5.7
PE(18 : 1/20 : 4)	8.07	P, N	0.79	1.6×10^{-3}	0.92	4.6×10^{-2}	0.9
PS(18 : 2/18 : 0)	8.08	N	—	—	1.28	1.3×10^{-3}	5.8
PS(18 : 0/20 : 3)	8.10	P	—	—	1.44	1.5×10^{-4}	7.9
PI(18 : 0/20 : 3)	8.13	N	0.38	3.3×10^{-2}	—	—	1.5
PC(16 : 1/16 : 1)	8.18	P	0.78	2.8×10^{-2}	—	—	6.3
PPE(18 : 1/22 : 6)	8.20	N	—	—	0.86	4.2×10^{-2}	2.5
PE(18 : 1/18 : 1)	8.22	P	0.75	4.7×10^{-3}	—	—	1.9
PC(16 : 0/22 : 6)	8.35	N	—	—	0.92	4.3×10^{-2}	4.0
PE(16 : 0/18 : 1)	8.38	P	0.82	3.7×10^{-2}	—	—	2.9
PC(16 : 0/20 : 4)	8.43	P, N	0.75	4.7×10^{-2}	0.89	4.5×10^{-2}	1.3
PC(16 : 1/16 : 0)	8.45	P	0.61	3.2×10^{-2}	0.74	2.4×10^{-2}	7.3
PPE(18 : 0/22 : 6)	8.48	N	—	—	0.89	1.3×10^{-2}	4.4
PPC(18 : 1/22 : 6)	8.62	P, N	—	—	0.69	7.6×10^{-3}	2.9
PE(18 : 1/18 : 0)	8.68	P	0.82	3.8×10^{-2}	0.79	4.0×10^{-2}	5.6
PE(18 : 0/22 : 4)	8.68	P	—	—	0.85	2.9×10^{-2}	6.5
PC(16 : 0/16 : 0)	8.80	N	—	—	0.86	2.2×10^{-2}	2.2
PC(18 : 0/22 : 6)	8.80	N	1.38	5.9×10^{-5}	—	—	4.6
PC(18 : 0/20 : 4)	8.88	N	—	—	0.89	4.1×10^{-2}	6.4
PC(18 : 2/18 : 0)	9.02	N	1.35	4.8×10^{-3}	—	—	2.9
PC(18 : 0/22 : 5)	9.10	N	—	—	0.84	2.9×10^{-2}	7.9
PC(18 : 0/20 : 3)	9.15	N	—	—	0.86	3.7×10^{-2}	6.9
PPC(18 : 0/16 : 0)	9.23	N	—	—	0.88	3.2×10^{-2}	1.5

Abbreviations: LPC, lyso-phosphocholine; LPS, lyso-phosphoserine; LPE, lyso-phosphoethanolamine; PG, phosphoglycerol; PS, phosphoserine; PI, phosphoinositol; PE, phosphoethanolamine; PC, phosphocholine; PPE, plasmenylethanolamine; PPC, plasmenylcholine.

described in the literature are based on the analysis of biofluids for the discovery of potential biomarkers for diagnosis, including cerebrospinal fluid,[38,39] blood samples,[40–43] urine[44,45] and saliva.[46] However, the study of peripheral organs that could be systemically affected has not been previously addressed. For this reason, the aim of this work was the characterization of the hepatic and renal metabolomic profiles in the APP/PS1 model of AD for the evaluation of possible implications of these metabolically active organs in the development of disease. To this end, we selected 6 months-old APP/PS1 mice, a transgenic model that reproduces well some of the neuropathological and behavioral deficits observed in human Alzheimer, with a phenotype characterized by deposition of Aβ plaques starting from the age of four months, glial activation, and deficits in cognitive functions at the age of 6 months.[17] Furthermore, previous metabolomic investigations in different biological compartments of this transgenic model showed numerous metabolic alterations, similar to those described in Tables 2–4, affecting brain[18,19] and serum samples.[47,48]

One of the most remarkable results could be associated with severe bioenergetic impairments, regarding altered levels of numerous energy-related metabolites listed in Tables 3 and 4. The decrease of several intermediates from glycolysis and pentose phosphate pathway (glucose, lactic acid, glucose-6-phosphate, fructose-6-phosphate, sedoheptulose-7-phosphate

Table 3 Other lipids identified as potential markers for discrimination between APP/PS1 and control mice

Metabolite	RT (min)	Ion mode	Liver		Kidney		RSD (%)
			Fold change	*p*-value	Fold change	*p*-value	
Sphingomyelins							
SM(d18 : 1/16 : 1)	7.90	N	—	—	0.82	3.7×10^{-2}	7.6
SM(d18 : 1/21 : 0)	9.55	P	—	—	1.49	3.2×10^{-2}	5.2
SM(d18 : 1/23 : 1)	9.65	P	—	—	1.70	3.7×10^{-2}	10.0
SM(d18 : 0/22 : 0)	9.77	P	—	—	1.83	6.3×10^{-3}	3.4
SM(d18 : 1/23 : 0)	10.07	P	—	—	1.76	4.2×10^{-2}	10.8
Ceramides							
CER(d18 : 1/24 : 1)	9.07	N	—	—	0.79	3.8×10^{-2}	4.2
Hex-CER(d18 : 1/24 : 0)	9.18	P	—	—	0.73	4.1×10^{-2}	3.2
Acylcarnitines							
C2-Car	0.32	P	—	—	0.71	2.3×10^{-3}	4.2
C4-OH-Car	0.33	P	0.49	1.0×10^{-6}	—	—	5.1
C3-Car	0.47	P	1.49	7.2×10^{-5}	—	—	3.9
C5-Car	2.12	P	1.51	4.2×10^{-3}	—	—	5.5
C10 : 0-Car	3.33	P	—	—	0.76	1.2×10^{-2}	9.0
C14 : 1-Car	3.77	P	—	—	0.78	1.6×10^{-3}	1.9
C14 : 0-Car	4.03	P	—	—	0.71	1.0×10^{-3}	2.8
C16 : 1-Car	4.17	P	0.73	7.8×10^{-3}	0.58	4.6×10^{-3}	8.9
C18 : 1-OH-Car	4.25	P	—	—	0.69	1.4×10^{-4}	9.1
C18 : 1-Car	4.70	P	0.63	2.6×10^{-3}	0.69	4.1×10^{-2}	3.3
C18 : 0-Car	5.22	P	0.66	2.7×10^{-2}	—	—	6.2
Steroids							
Taurocholic acid	3.08	P, N	0.33	7.6×10^{-4}	—	—	4.8
Taurodeoxycholic acid	3.22	N	0.29	3.5×10^{-3}	—	—	2.8
Sulfolithocholylglycine	3.30	N	0.40	1.0×10^{-2}	—	—	2.2
Glycocholic acid	3.38	N	0.24	8.2×10^{-4}	—	—	6.8
Cholesterol	16.17	EI	2.18	1.7×10^{-3}	—	—	4.4
Campesterol	16.83	EI	1.60	9.3×10^{-3}	1.72	1.8×10^{-5}	6.3
Fatty acids							
Oleic acid	11.03	EI	0.81	4.1×10^{-3}	—	—	1.8
Stearic acid	11.08	EI	1.19	3.7×10^{-3}	1.16	8.5×10^{-3}	2.9
Arachidonic acid	11.95	EI	0.67	3.9×10^{-3}	—	—	2.2

Abbreviations: SM, sphingomyelin, CER, ceramide; Hex-CER, hexosyl-ceramide; Car, carnitine.

and 1,3-bisphosphoglycerate), together with the increase of sucrose levels support a perturbed metabolism of carbohydrates. Moreover, mitochondrial abnormalities were also observed considering the accumulation of succinic and malic acids, involved in Krebs cycle. These findings agree with the proven hypothesis of hypometabolism in AD brains, caused by a decline in glucose utilization and mitochondrial dysfunction,[49] but here it is demonstrated for the first time that this situation is widespread throughout the whole organism affecting peripheral organs such as liver and kidney. There is also growing evidence that metabolic syndrome, a constellation of metabolic risk factors related to cerebrovascular disease and diabetes mellitus that includes impaired glucose tolerance, dyslipidemia or hypertension, may play an important role in the development of Alzheimer's disease.[50] In this sense, in this study we found a significant increase of renal sorbitol that might denote impaired polyol pathway, one of the major metabolic changes leading to diabetic neuropathy.[51] Furthermore, the acylcarnitine pattern observed by UHPLC-MS profiling (Table 3) showed close similarities to those described for patients affected by metabolic syndrome, type 1 diabetes and type 2 diabetes, with reduced content of long chain acylcarnitines and increased levels of short chain species.[52] The reduction of most acylcarnitines in both liver and kidney suggests a perturbed transport of fatty acids into the mitochondria for β-oxidation, which is in accordance with previous studies that showed lower levels of L-carnitine in AD patients,[33,38,42,43] together with altered expression of several related enzymes such as decreased carnitine acetyltransferase activity,[53] or over-expressed hydroxyacyl-coenzyme A dehydrogenase[54] and short chain 3-hydroxyacyl-CoA dehydrogenase.[55] By contrast odd-chain acylcarnitines (propionyl- and pivaloylcarnitine), derived from the catabolism of branched chain amino acids, were increased in liver tissue, which is known to be a contributing factor to insulin resistance.[56] Finally, the overall decrease of different amino acids (alanine, glutamine, glutamate, valine, threonine and glycine) may indicate enhanced gluconeogenesis, a metabolic pathway exclusively expressed in liver and kidney for synthesizing glucose. Therefore, impaired systemic energy metabolism stands out as a central mechanism leading to pathogenesis in the APP/PS1 mice, comprising failures in glycolysis, Krebs cycle, β-oxidation, gluconeogenesis and several hallmarks of metabolic syndrome not previously described for Alzheimer's disease such as altered polyol pathway and catabolism of branched chain amino acids.

Table 4 Low molecular weight metabolites identified as potential markers for discrimination between APP/PS1 and control mice

Metabolite	RT (min)	Ion mode	Liver		Kidney		RSD (%)
			Fold change	*p*-value	Fold change	*p*-value	
Lactic acid	2.65	EI	0.72	3.9×10^{-2}	0.61	4.0×10^{-2}	6.8
Alanine	2.97	EI	0.78	2.7×10^{-2}	0.90	2.7×10^{-3}	3.9
Urea	3.93	EI	0.54	3.5×10^{-3}	—	—	10.4
Glycerol	4.03	EI	2.35	6.1×10^{-4}	—	—	8.8
Glycine	4.37	EI	0.59	4.8×10^{-4}	0.89	2.2×10^{-2}	8.3
Succinic acid[a]	4.42,[b] 0.30[c]	EI, N	1.73	1.9×10^{-4}	—	—	1.8
Malic acid[a]	5.82,[b] 0.30[c]	EI, N	1.58	1.6×10^{-2}	—	—	6.0
Pyroglutamic acid	6.12	EI	0.50	1.1×10^{-3}	0.52	2.3×10^{-3}	5.5
Glutamic acid	6.88	EI	0.74	3.6×10^{-2}	0.75	3.2×10^{-2}	7.3
Glycerol-3-phosphate	7.80	EI	1.41	2.7×10^{-2}	1.31	1.7×10^{-2}	3.3
Phosphoethanolamine	8.12	EI	1.69	3.4×10^{-2}	1.38	1.4×10^{-2}	6.5
Glucose[a]	8.87,[b] 0.30[c]	EI, N	0.64	2.6×10^{-4}	0.43	1.5×10^{-4}	4.8
Sorbitol	9.08	EI	—	—	1.45	2.5×10^{-3}	3.3
Myoinositol	10.10	EI	—	—	1.42	1.9×10^{-3}	9.2
Uric acid	10.23	EI	0.65	3.3×10^{-2}	—	—	5.1
Myoinositol-1-phosphate	10.90	EI	—	—	1.31	6.4×10^{-3}	10.1
Fructose-6-phosphate	11.40	EI	0.80	2.9×10^{-2}	—	—	8.6
Glucose-6-phosphate	11.47	EI	0.79	4.0×10^{-2}	—	—	7.3
Sedoheptulose-7-phosphate	12.73	EI	0.85	3.6×10^{-2}	—	—	11.9
1,3-Bisphosphoglycerate	15.38	EI	0.79	4.0×10^{-2}	—	—	9.0
Choline	0.30	P	1.77	1.0×10^{-6}	—	—	1.9
Phosphocholine	0.30	P, N	2.16	4.0×10^{-6}	1.34	1.4×10^{-2}	1.4
Glycerophosphocholine	0.30	P, N	1.41	6.7×10^{-5}	—	—	7.1
Valine	0.30	P	0.65	7.9×10^{-4}	—	—	5.5
Threonine	0.30	N	—	—	0.80	3.4×10^{-2}	5.1
Glutamine	0.30	N	—	—	0.85	1.4×10^{-2}	1.1
Spermidine	0.30	P	1.59	4.1×10^{-3}	—	—	9.1
Ergothioneine	0.30	P	1.49	2.3×10^{-3}	1.62	3.0×10^{-6}	8.9
Sucrose	0.30	N	1.65	8.9×10^{-3}	—	—	6.8

[a] Metabolites detected complementarily by GC-MS and UHPLC-MS. [b] Retention time for GC-MS. [c] Retention time for UHPLC-MS.

Metabolism of phospholipids was also significantly perturbed in peripheral organs of the APP/PS1 mice, with altered levels of numerous compounds including phosphocholines (PC), phosphoethanolamines (PE), plasmalogens (PPC and PPE), phosphoinositols (PI), phosphoserines (PS), phosphoglycerols (PG), lyso-phospholipids and other catabolic metabolites (Tables 2 and 4). Membrane breakdown is a key pathological mechanism occurring in the AD brain, which has been traditionally associated with over-activation of phospholipases, principally phospholipase A_2 (PLA_2), leading to phospholipid degradation and resulting in the generation of second messengers involved in neurodegeneration.[57] Thus, previous investigations in the postmortem brain of AD patients showed decreased total levels of phospholipids[58] and the accumulation of catabolic intermediates.[59] Similarly, numerous byproducts resulting from the degradation of phospholipids were elevated in liver and kidney of APP/PS1 mice (Table 4), including glycerophosphocholine, phosphocholine, phosphoethanolamine and choline, as well as the final products of this degradation process, glycerol-3-phosphate and free glycerol, corroborating that degradation of membrane lipids is not exclusively localized in brain tissue. Moreover, profound alterations were observed in phospholipids species, which depended on the type of fatty acid linked to the molecular moiety, the phospholipid class and the tissue considered. In liver, the main changes can be attributed to reduced content of phospholipids, most of them containing polyunsaturated fatty acids in their structure (principally arachidonic and docosahexaenoic acids). In this sense, González-Domínguez *et al.* recently hypothesized that membrane destabilization processes in AD are associated with imbalances in the levels of saturated/unsaturated fatty acids, which support an implication of oxidative stress in this progressive degradation.[27,42,60] However, specific phospholipid species containing stearic acid were increased in this tissue, suggesting an abnormal metabolism of this fatty acid. Previous studies revealed altered expression of stearoyl-CoA desaturase in brains of patients with Alzheimer's disease, the rate-limiting enzyme in biosynthesis of monounsaturated fatty acids from stearic acid.[61] Thereby, the accumulation of stearic acid could lead to a profound membrane remodeling, because this is one of the most abundant fatty acids forming phospholipids. Interestingly, a similar trend was observed for lyso-phospholipids and free fatty acids generated by hydrolysis of the ester bonds from phospholipids by the action of PLA_2, with increased levels of stearic-derived compounds and decreased content of other lipids (Tables 2 and 3). On the other hand, major phospholipids species were decreased in kidney independently of the fatty acid composition, including phosphocholines, phosphoethanolamines and plasmalogens, corroborating an increased turnover of phospholipids. Nevertheless, a parallel increase was observed for less abundant phospholipids such as phosphoglycerols, phosphoserines and phosphoinositols, which could have important implications in AD pathogenesis. Phosphoglycerols are precursors of cardiolipin, an essential phospholipid for mitochondrial function that is

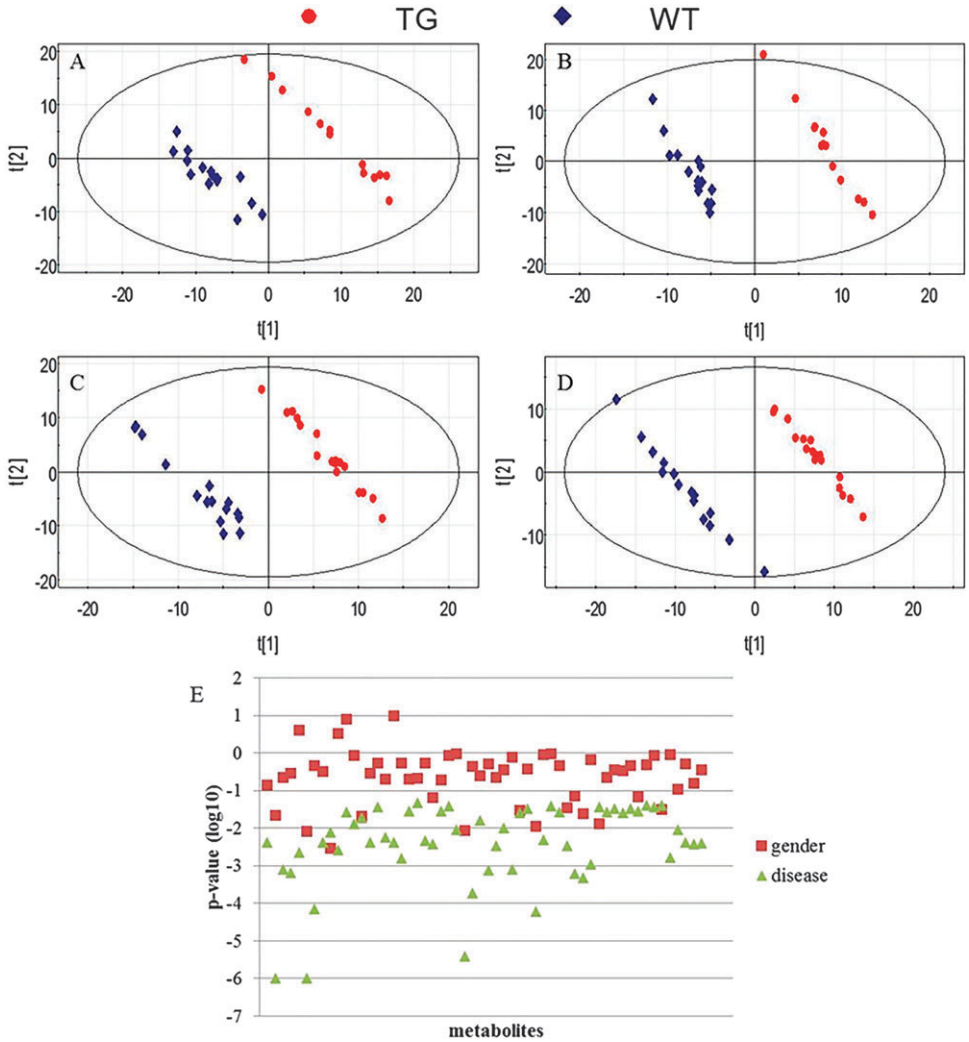

Fig. 3 Assessment of gender-related differences on metabolomic profiles. (A–D) PLS-DA plots of statistical models for UHPLC-ESI(+)-MS data. (A) Liver (male); (B) kidney (male); (C) liver (female); (D) kidney (female). (E) Comparison of *p*-values for potential markers listed in Tables 2–4 with *p*-values according to gender for these metabolites.

decreased in AD brain.[62] Alternatively, the increase of phosphoserines has been previously described in brains,[63] which have a prominent role in maintaining asymmetric distribution of phospholipids in membranes. Finally, increased levels of phosphoinositols as well as related metabolites myoinositol and myoinositol-1-phosphate (Table 4) may be directly related to altered phosphatidylinositol metabolism and dysfunctions in the phosphoinositide signaling system.[64]

Besides these alterations in levels of phospholipids, metabolism of sphingolipids was also impaired (only in kidney) corroborating a perturbed homeostasis of cellular membranes (Table 3). Sphingolipids are bioactive compounds in lipid membrane rafts that may act as signaling molecules involved in the regulation of cell growth, differentiation, senescence and apoptosis, which participate in a pivotal event in the dysfunction of neurons in Alzheimer's disease.[65] Similar to phospholipids, a different trend was observed depending on the fatty acid composition, with a significant increase of sphingomyelins containing very long chain fatty acids and the decrease of short chain ones. This change in the acyl chain length of sphingolipids has a great importance in their biophysical properties, which may have a pathological impact on Alzheimer's disease.[66] Moreover, this increase of long chain sphingomyelins was accompanied by a decrease of related ceramides, supporting a shift in metabolism of sphingolipids as previously reported in AD brain.[67] Therefore, cellular membranes could be considered as primary targets in pathogenesis of AD in the APP/PS1 transgenic mice, in both the central nervous system and the peripheral organs.

Elevated cholesterol content in liver (Table 3) suggests a situation of hyperlipidemia, one of the most important vascular risk factors that have been associated with the development of Alzheimer's disease.[68] In addition, the decrease of different bile acids in the same tissue (taurocholic acid, taurodeoxycholic acid, sulfolithocholylglycine and glycocholic acid) may indicate a profound deregulation of steroid homeostasis. Urea is produced in the liver by means of the urea cycle in order to remove ammonia from the organism, whose accumulation may lead to hepatic encephalopathy that results in severe central nervous

system dysfunction.[69] Thereby, the hepatic reduction of urea levels (Table 4) points to perturbed regulation of the urea cycle, in agreement with previous studies showing enzymatic abnormalities[70] and altered content of related metabolites.[41,60] Decreased levels of uric acid and pyroglutamate could be considered as systemic markers of oxidative stress, an important hallmark of Alzheimer's disease.[2] Uric acid is one of the most common antioxidants, and its reduction in plasma has been previously reported in AD.[71] Moreover, pyroglutamic acid is involved in biosynthesis of other important antioxidant as is glutathione, so its reduction may be associated with problems in glutathione metabolism.[14] Metabolomic profiling also revealed a significant increase of two exogenous compounds, ergothioneine and campesterol, in both liver and kidney. Ergothioneine, synthesized from histidine in organisms such as actinobacteria or filamentous fungi, presents antioxidant properties, while campesterol is a phytosterol with anti-inflammatory effects. Since no endogenous synthesis pathways are known for these compounds, the accumulation observed in our study must be due to enhanced uptake from the diet. In this sense, McClay *et al.* found that ergothioneine levels increased in brain of mice following repeated methamphetamine exposure, presumably in response to oxidative stress.[72] On the other hand, elevated campesterol might be explained by up-regulated expression of ABC transporters, responsible for cellular absorption of cholesterol and phytosterols. Finally, liver from APP/PS1 mice showed higher spermidine levels (Table 4), a multifunctional polyamine involved in NMDA–receptor regulation. In this context, amyloid beta deposition is known to up-regulate polyamine metabolism in Alzheimer's disease by increasing ornithine decarboxylase activity and polyamine uptake, leading to altered levels of polyamines in brain,[34] which confirms our metabolomic findings on liver.

3.4. Comparison with brain alterations

Metabolomic changes observed in liver and kidney tissues (Tables 2–4) were compared with brain alterations in these transgenic animals in order to evaluate metabolic similarities and differences between the central nervous system and the peripheral system from the APP/PS1 mouse model. The analysis of brain samples from APP/PS1 and wild-type mice studied in this work has been previously performed using the same metabolomic multi-platform based on GC-MS and RP-UHPLC-MS,[18] as well as by using direct infusion mass spectrometry.[19] These studies demonstrated that hippocampus and cortex are the most perturbed brain regions in this transgenic model, but cerebellum, striatum and olfactory bulbs are also affected to a lesser extent. The comparison of metabolite profiles from liver, kidney and brain regions showed similar alterations in numerous compounds, thus demonstrating the systemic nature of pathological mechanisms underlying these metabolic abnormalities. In this sense, it should be noted that all these biological compartments were affected by significant failures in different pathways involved in the bioenergetic metabolism, including reduced carbohydrate utilization, impaired mitochondrial function (*e.g.* Krebs cycle), perturbed lipid metabolism by means of β-oxidation, and disturbed phosphocreatine system. Furthermore, the change in fatty acid composition of phospholipids described in the previous section for liver and kidney was also observed in brain from these transgenic animals, with a considerable reduction of species derived from polyunsaturated fatty acids and a parallel increase of saturated ones, especially those derived from stearic acid. Levels of urea and related metabolites were decreased in both the central nervous system and the peripheral organs studied in the present work, together with increased content of polyamines, suggesting important failures in the homeostasis of ammonia leading to hiperammonemia. Finally, we also observed that oxidative stress might play a prominent role in pathogenesis of AD affecting the whole organism, with reduced levels of different antioxidant compounds (*e.g.* glutathione, uric acid, homocarnosine) in all biological tissues analyzed. On the other hand, it is noteworthy that some metabolites showed opposite trends in different tissues, which could be indicative of the existence of selective alterations depending on the organ studied. Thereby, we detected a significant imbalance in levels of sphingomyelins containing very long chain fatty acids, whose concentration was decreased in brain tissue but increased in kidneys, evidencing that metabolism of these sphingolipids is regulated in a different manner in the central nervous system and the peripheral system. Moreover, reduced content of cholesterol was observed in brain from these transgenic animals,[18] indicative of serious alterations of the physicochemical structure of lipid rafts. However, cholesterol levels were increased in peripheral samples, which suggests a situation of hyperlipidemia. Therefore, it could be concluded that pathological mechanisms associated with AD-type disorders in the APP/PS1 model provoke significant metabolic alterations affecting the whole organism, including different brain regions and peripheral organs such as liver and kidneys, most of them common to all the biological compartments studied, while other abnormalities showed a differential regulation depending on the tissue considered.

4. Conclusions

In this study for the first time we demonstrated that important metabolomic alterations occur in the liver and kidney of the APP/PS1 transgenic mice with Alzheimer's disease. For this purpose, a high-throughput metabolomic multiplatform was employed based on simple tissue homogenization and fast analysis by complementary gas chromatography-mass spectrometry and reversed-phase ultra-high performance liquid chromatography-mass spectrometry. Thereby, we observed that some key neuronal features of Alzheimer's disease are widespread to peripheral organs, including impaired glucose metabolism, mitochondrial dysfunction, abnormal metabolism of membrane lipids, or oxidative stress, among others. Moreover, novel pathological mechanisms were found such as impaired gluconeogenesis, polyol pathway or metabolism of branched chain amino acids, not previously described in other studies

using brain or biofluids. Therefore, these findings clearly support the hypothesis that Alzheimer's disease may be a systemic disorder. As a future plan, it would be interesting to extend this research line to other organs, such as the pancreas, involved in the regulation of insulin secretion, for the characterization of the systemic character of this neurodegenerative disorder in a more comprehensive manner.

Acknowledgements

This work was supported by the projects CTM2012-38720-C03-01 from the Ministerio de Ciencia e Innovación and P008-FQM-3554 and P009-FQM-4659 from the Consejería de Innovación, Ciencia y Empresa (Junta de Andalucía). Raúl González Domínguez thanks the Ministerio de Educación for a predoctoral scholarship (AP2010-4278).

References

1 D. J. Selkoe, *Nature*, 2003, **426**, 900–904.
2 M. A. Smith, C. A. Rottkamp, A. Nunomura, A. K. Raina and G. Perry, *Biochim. Biophys. Acta*, 2000, **1502**, 139–144.
3 E. E. Tuppo and H. R. Arias, *Int. J. Biochem. Cell Biol.*, 2005, **37**, 289–305.
4 A. Maruszak and C. Żekanowski, *Prog. Neuro-Psychopharmacol. Biol. Psychiatry*, 2011, **35**, 320–330.
5 C. L. Joachim, H. Mori and D. J. Selkoe, *Nature*, 1989, **341**, 226–230.
6 A. E. Roher, C. L. Esh, T. A. Kokjohn, E. M. Castaño, G. D. Van Vickle, W. M. Kalback, R. L. Patton, D. C. Luehrs, I. D. Daugs, Y. M. Kuo, M. R. Emmerling, H. Soares, J. F. Quinn, J. Kaye, D. J. Connor, N. B. Silverberg, C. H. Adler, J. D. Seward, T. G. Beach and M. N. Sabbagh, *Alzheimer's Dementia*, 2009, **5**, 18–29.
7 C. Holmes, *Neuropathol. Appl. Neurobiol.*, 2013, **39**, 51–68.
8 C. Cervellati, E. Cremonini, C. Bosi, S. Magon, A. Zurlo, C. M. Bergamini and G. Zuliani, *Curr. Alzheimer Res.*, 2013, **10**, 365–372.
9 V. Giordano, G. Peluso, M. Iannuccelli, P. Benatti, R. Nicolai and M. Calvani, *Neurochem. Res.*, 2007, **32**, 555–567.
10 R. González-Domínguez, T. García-Barrera and J. L. Gómez-Ariza, *BioMetals*, 2014, **26**, 539–549.
11 R. González-Domínguez, T. García-Barrera and J. L. Gómez-Ariza, *Metallomics*, 2014, **6**, 292–300.
12 R. Squitti, *Front. Biosci.*, 2012, **17**, 451–472.
13 G. Astarita and D. Piomelli, *Prostaglandins, Leukotrienes Essent. Fatty Acids*, 2011, **85**, 197–203.
14 K. Aoyama and T. Nakaki, *Int. J. Mol. Sci.*, 2013, **14**, 21021–21044.
15 J. Kou, G. G. Kovacs, R. Höftberger, W. Kulik, A. Brodde, S. Forss-Petter, S. Hönigschnabl, A. Gleiss, B. Brügger, R. Wanders, W. Just, H. Budka, S. Jungwirth, P. Fischer and J. Berger, *Acta Neuropathol.*, 2011, **122**, 271–283.
16 M. Mogi and M. Horiuchi, *Cardiol. Res. Pract.*, 2011, **2011**, 306189.
17 T. Malm, J. Koistinaho and K. Kanninen, *Int. J. Alzheimer's Dis.*, 2011, **2011**, 517160.
18 R. González-Domínguez, T. García-Barrera, J. Vitorica and J. L. Gómez-Ariza, *Biochim. Biophys. Acta, Mol. Basis Dis.*, 2014, **1842**, 2395–2402.
19 R. González-Domínguez, T. García-Barrera, J. Vitorica and J. L. Gómez-Ariza, *J. Pharm. Biomed. Anal.*, 2015, **102**, 425–435.
20 K. Dettmer, P. A. Aronov and B. D. Hammock, *Mass Spectrom. Rev.*, 2007, **26**, 51–78.
21 J. L. Jankowsky, D. J. Fadale, J. Anderson, G. M. Xu, V. Gonzales, N. A. Jenkins, N. G. Copeland, M. K. Lee, L. H. Younkin, S. L. Wagner, S. G. Younkin and D. R. Borchelt, *Hum. Mol. Genet.*, 2004, **13**, 159–170.
22 T. Sangster, H. Major, R. Plumb, A. J. Wilson and I. D. Wilson, *Analyst*, 2006, **131**, 1075–1078.
23 M. Katajamaa and M. Oresic, *J. Chromatogr. A*, 2007, **1158**, 318–328.
24 C. A. Smith, E. J. Want, G. O'Maille, R. Abagyan and G. Siuzdak, *Anal. Chem.*, 2006, **78**, 779–787.
25 K. A. Veselkov, L. K. Vingara, P. Masson, S. L. Robinette, E. Want, J. V. Li, R. H. Barton, C. Boursier-Neyret, B. Walther, T. M. Ebbels, I. Pelczer, E. Holmes, J. C. Lindon and J. K. Nicholson, *Anal. Chem.*, 2011, **83**, 5864–5872.
26 R. A. van den Berg, H. C. J. Hoefsloot, J. A. Westerhuis, A. K. Smilde and M. J. van der Werf, *BMC Genomics*, 2006, **7**, 142.
27 R. Gonzalez-Dominguez, T. Garcia-Barrera and J. L. Gomez-Ariza, *J. Proteomics*, 2014, **104**, 37–47.
28 C. A. Haynes, J. C. Allegood, H. Park and M. C. Sullards, *J. Chromatogr. B: Anal. Technol. Biomed. Life Sci.*, 2009, **877**, 2696–2708.
29 L. Vernez, G. Hopfgartner, M. Wenk and S. Krahenbuhl, *J. Chromatogr. A*, 2003, **984**, 203–213.
30 S. Naz, M. Vallejo, A. García and C. Barbas, *J. Chromatogr. A*, 2014, **1353**, 99–105.
31 C. T. Viswanathan, S. Bansal, B. Booth, A. J. DeStefano, M. J. Rose, J. Sailstad, V. P. Shah, J. P. Skelly, P. G. Swann and R. Weiner, *Pharm. Res.*, 2007, **24**, 1962–1973.
32 J. Zhang, L. Yan, M. Tian, Q. Huang, S. Peng, S. Dong and H. Shen, *J. Pharm. Biomed. Anal.*, 2012, **66**, 287–297.
33 S. F. Graham, C. Holscher and B. D. Green, *Metabolomics*, 2014, **10**, 744–753.
34 K. Inoue, H. Tsutsui, H. Akatsu, Y. Hashizume, N. Matsukawa, T. Yamamoto and T. Toyo'oka, *Sci. Rep.*, 2013, **3**, 2364.
35 S. F. Graham, C. Holscher, P. McClean, C. T. Elliott and B. D. Green, *Metabolomics*, 2013, **9**, 974–983.
36 R. M. Salek, J. Xia, A. Innes, B. C. Sweatman, R. Adalbert, S. Randle, E. McGowan, P. C. Emson and J. L. Griffin, *Neurochem. Int.*, 2010, **56**, 937–943.
37 Z. P. Hu, E. R. Browne, T. Liu, T. E. Angel, P. C. Ho and E. C. Y. Chan, *J. Proteome Res.*, 2012, **11**, 5903–5913.
38 C. Ibáñez, C. Simó, P. J. Martín-Álvarez, M. Kivipelto, B. Winblad, A. Cedazo-Mínguez and A. Cifuentes, *Anal. Chem.*, 2012, **84**, 8532–8540.
39 C. Ibáñez, C. Simó, D. K. Barupal, O. Fiehn, M. Kivipelto, A. Cedazo-Mínguez and A. Cifuentes, *J. Chromatogr. A*, 2013, **1302**, 65–71.

40 G. Wang, Y. Zhou, F. J. Huang, H. D. Tang, X. H. Xu, J. J. Liu, Y. Wang, Y. L. Deng, R. J. Ren, W. Xu, J. F. Ma, Y. N. Zhang, A. H. Zhao, S. D. Chen and W. Jia, *J. Proteome Res.*, 2014, **13**, 2649–2658.
41 R. González-Domínguez, T. Garcia-Barrera and J. L. Gomez-Ariza, *Talanta*, 2015, **131**, 480–489.
42 R. González-Domínguez, T. García-Barrera and J. L. Gómez-Ariza, *Anal. Bioanal. Chem.*, 2014, **406**, 7137–7148.
43 R. González-Domínguez, A. García, T. García-Barrera, C. Barbas and J. L. Gómez-Ariza, *Electrophoresis*, 2014, **35**, 3321–3330.
44 K. Fukuhara, A. Ohno, Y. Ota, Y. Senoo, K. Maekawa, H. Okuda, M. Kurihara, A. Okuno, S. Niida, Y. Saito and O. Takikawa, *J. Clin. Biochem. Nutr.*, 2013, **52**, 133–138.
45 R. Gonzalez-Dominguez, R. Castilla-Quintero, T. Garcia-Barrera and J. L. Gomez-Ariza, *Anal. Biochem.*, 2014, **465**, 20–27.
46 M. Tsuruoka, J. Hara, A. Hirayama, M. Sugimoto, T. Soga, W. R. Shankle and M. Tomita, *Electrophoresis*, 2013, **34**, 2865–2872.
47 R. González-Domínguez, T. García-Barrera, J. Vitorica and J. L. Gómez-Ariza, *J. Pharm. Biomed. Anal.*, 2015, **107**, 378–385.
48 R. González-Domínguez, T. García-Barrera, J. Vitorica and J. L. Gómez-Ariza, *Biochimie*, 2015, **110**, 119–128.
49 H. Atamna and W. H. Frey II, *Mitochondrion*, 2007, **7**, 297–310.
50 V. Frisardi, V. Solfrizzi, D. Seripa, C. Capurso, A. Santamato, D. Sancarlo, G. Vendemiale, A. Pilotto and F. Panza, *Ageing Res. Rev.*, 2010, **9**, 399–417.
51 P. Sytze Van Dam, M. A. Cotter, B. Bravenboer and N. E. Cameron, *Eur. J. Pharmacol.*, 2013, **719**, 180–186.
52 J. Bene, M. Márton, M. Mohás, Z. Bagosi, Z. Bujtor, T. Oroszlán, B. Gasztonyi, I. Wittmann and B. Melegh, *Ann. Nutr. Metab.*, 2013, **62**, 80–85.
53 T. K. Makar, A. J. Cooper, B. Tofel-Grehl, H. T. Thaler and J. P. Blass, *Neurochem. Res.*, 1995, **20**, 705–711.
54 J. Yao, R. T. Hamilton, E. Cadenas and R. D. Brinton, *Biochim. Biophys. Acta*, 2010, **1800**, 1121–1126.
55 S. Y. Yang, X. Y. He and H. Schulz, *FEBS J.*, 2005, **272**, 4874–4883.
56 C. B. Newgard, J. An, J. R. Bain, M. J. Muehlbauer, R. D. Stevens, L. F. Lien, A. M. Haqq, S. H. Shah, M. Arlotto, C. A. Slentz, J. Rochon, D. Gallup, O. Ilkayeva, B. R. Wenner, W. S. Yancy Jr, H. Eisenson, G. Musante, R. S. Surwit, D. S. Millington, M. D. Butler and L. P. Svetkey, *Cell Metab.*, 2009, **9**, 311–326.
57 A. A. Farooqui, W. Y. Ong and L. A. Horrocks, *Neurochem. Res.*, 2004, **29**, 1961–1977.
58 C. G. Gottfries, I. Karlsson and L. Svennerholm, *Int. Psychogeriatr.*, 1996, **8**, 365–372.
59 A. Walter, U. Korth, M. Hilgert, J. Hartmann, O. Weichel, M. Hilgert, K. Fassbender, A. Schmitt and J. Klein, *Neurobiol. Aging*, 2004, **25**, 1299–1303.
60 R. González-Domínguez, T. García-Barrera and J. L. Gómez-Ariza, *J. Pharm. Biomed. Anal.*, 2014, **98**, 321–326.
61 G. Astarita, K. M. Jung, V. Vasilevko, N. V. DiPatrizio, S. K. Martin, D. H. Cribbs, E. Head, C. W. Cotman and D. Piomelli, *PLoS One*, 2011, **6**, e24777.
62 J. W. Pettegrew, K. Panchalingam, R. L. Hamilton and R. J. McClure, *Neurochem. Res.*, 2001, **26**, 771–782.
63 A. A. Farooqui, S. I. Rapoport and L. A. Horrocks, *Neurochem. Res.*, 1997, **22**, 523–527.
64 C. J. Fowler, *Brain Res. Rev.*, 1997, **25**, 373–380.
65 G. V. Echten-Deckert and J. Walter, *Prog. Lipid Res.*, 2012, **51**, 378–393.
66 O. Ben-David and A. H. Futerman, *NeuroMol. Med.*, 2010, **12**, 341–350.
67 X. He, Y. Huang, B. Li, C. X. Gong and E. H. Schuchman, *Neurobiol. Aging*, 2010, **31**, 398–408.
68 M. A. Pappolla, T. Bryant-Thomas, D. Herbert, J. Pacheco, M. Fabra Garcia, M. Manjon, X. Girones, T. L. Henry, E. Matsubara, D. Zambon, B. Wolozin, M. Sano, F. F. Cruz-Sanchez, L. J. Thal, S. S. Petanceska and L. M. Refolo, *Neurology*, 2003, **61**, 199–205.
69 V. Felipo and R. F. Butterworth, *Prog. Neurobiol.*, 2002, **67**, 259–279.
70 F. Hansmannel, A. Sillaire, M. I. Kamboh, C. Lendon, F. Pasquier, D. Hannequin, G. Laumet, A. Mounier, A. M. Ayral, S. T. DeKosky, J. J. Hauw, C. Berr, D. Mann, P. Amouyel, D. Campion and J. C. Lambert, *J. Alzheimer's Dis.*, 2010, **21**, 1013–1021.
71 T. S. Kim, C. U. Pae, S. J. Yoon, W. Y. Jang, N. J. Lee, J. J. Kim, S. J. Lee, C. Lee, I. H. Paik and C. U. Lee, *Int. J. Geriatr. Psychopharmacol.*, 2006, **21**, 344–348.
72 J. L. McClay, D. E. Adkins, S. A. Vunck, A. M. Batman, R. E. Vann, S. L. Clark, P. M. Beardsley and E. J. C. G. van den Oord, *Metabolomics*, 2013, **9**, 392–402.